Global Biogeochemical Cycles®

RESEARCH ARTICLE
10.1029/2020GB006901

Isoscape Models of the Southern Ocean: Predicting Spatial and Temporal Variability in Carbon and Nitrogen Isotope Compositions of Particulate Organic Matter

Katie St John Glew[1], Boris Espinasse[2], Brian P. V. Hunt[3,4,5], Evgeny A. Pakhomov[3,4,5], Sarah J. Bury[6], Matt Pinkerton[6], Scott D. Nodder[6], Andres Gutiérrez-Rodríguez[6], Karl Safi[7], Julie C. S. Brown[6], Laura Graham[8,9], Robert B. Dunbar[10], David A. Mucciarone[10], Sarah Magozzi[11], Chris Somes[12], and Clive N. Trueman[1,13]

[1]School of Ocean and Earth Science, University of Southampton, National Oceanography Centre Southampton, Southampton, UK, [2]Department of Arctic and Marine Biology, UiT The Arctic University of Norway, Tromsø, Norway, [3]Institute for the Oceans and Fisheries, University of British Columbia, Vancouver, BC, Canada, [4]Department of Earth, Ocean and Atmospheric Sciences, University of British Columbia, Vancouver, BC, Canada, [5]Hakai Institute, Tula Foundation, Heriot Bay, BC, Canada, [6]National Institute of Water & Atmospheric Research Ltd (NIWA), Wellington, New Zealand, [7]National Institute of Water & Atmospheric Research Ltd (NIWA), Hamilton, New Zealand, [8]Geography, Earth and Environmental Sciences, University of Birmingham, Birmingham, UK, [9]Biodiversity, Ecology and Conservation Group, International Institute for Applied Systems Analysis, Laxenburg, Austria, [10]Earth System Science, Stanford University, Stanford, CA, USA, [11]Department of Integrative Marine Ecology, Stazione Zoologica Anton Dohrn, Fano Marine Centre, Fano, Italy, [12]Marine Biogeochemical Modelling, GEOMAR Helmholtz Centre for Ocean Research Kiel, Kiel, Germany, [13]Hong Kong Branch of Southern Marine Science and Engineering Guangdong Laboratory (Guangzhou), Hong Kong, China

Abstract Polar marine ecosystems are particularly vulnerable to the effects of climate change. Warming temperatures, freshening seawater, and disruption to sea-ice formation potentially all have cascading effects on food webs. New approaches are needed to better understand spatiotemporal interactions among biogeochemical processes at the base of Southern Ocean food webs. In marine systems, isoscapes (models of the spatial variation in the stable isotopic composition) of carbon and nitrogen have proven useful in identifying spatial variation in a range of biogeochemical processes, such as nutrient utilization by phytoplankton. Isoscapes provide a baseline for interpreting stable isotope compositions of higher trophic level animals in movement, migration, and diet research. Here, we produce carbon and nitrogen isoscapes across the entire Southern Ocean (>40°S) using surface particulate organic matter isotope data, collected over the past 50 years. We use Integrated Nested Laplace Approximation-based approaches to predict mean annual isoscapes and four seasonal isoscapes using a suite of environmental data as predictor variables. Clear spatial gradients in $\delta^{13}C$ and $\delta^{15}N$ values were predicted across the Southern Ocean, consistent with previous statistical and mechanistic views of isotopic variability in this region. We identify strong seasonal variability in both carbon and nitrogen isoscapes, with key implications for the use of static or annual average isoscape baselines in animal studies attempting to document seasonal migratory or foraging behaviors.

St John Glew and B. Espinasse are joint first author.

Key Points:

- First carbon and nitrogen isoscape predictions of the entire Southern Ocean, based on particulate organic matter isotope data
- Clear spatial gradients in $\delta^{13}C$ and $\delta^{15}N$ values were predicted, consistent with previously reported isotopic variability in this region
- Key implications for the use of isoscape baselines in animal studies attempting to document seasonal migratory or foraging behaviors

Supporting Information:

Supporting Information may be found in the online version of this article.

Correspondence to:

B. Espinasse,
boris.espinasse@laposte.net

Citation:

St John Glew, K., Espinasse, B., Hunt, B. P. V., Pakhomov, E. A., Bury, S. J., Pinkerton, M., et al. (2021). Isoscape models of the Southern Ocean: Predicting spatial and temporal variability in carbon and nitrogen isotope compositions of particulate organic matter. *Global Biogeochemical Cycles*, *35*, e2020GB006901. https://doi.org/10.1029/2020GB006901

Received 27 NOV 2020
Accepted 11 AUG 2021

1. Introduction

Polar marine ecosystems are impacted disproportionately by ongoing climate change, with observations showing significant ocean warming and freshening trends over several recent decades (Durack & Wijffels, 2010; Henley et al., 2020; Schofield et al., 2010; Swart et al., 2018). Warming ocean temperatures directly affect sea-ice production and melting rates which play a crucial role in the life cycles of many polar marine animals (Loeb et al., 1997). Further, both warming and freshening affect water column structure (stratification, mixing) and dominant biogeochemical processes supporting primary productivity of these regions (Deppeler & Davidson, 2017; Li et al., 2009). Such disruptions at the base of the trophic food web can potentially have large-scale consequences throughout the ecosystem (Henley et al., 2020), and there is a need to better understand spatiotemporal interactions among biogeochemical processes at regional scales.

The Southern Ocean (>40°S) surrounds the Antarctic continent and contains around 15% of the world's ocean surface area, with variable sea-ice cover that results in large marginal ice zones (MIZs). The dominant

feature of the Southern Ocean is the eastward flowing Antarctic Circumpolar Current, characterized by a latitudinal gradient in temperature with sharp changes across fronts, separating regions with relatively homogenous physical and chemical properties (Henley et al., 2020; Orsi & Harris, 2019). The Southern Ocean is a High Nutrient Low Chlorophyll (HNLC) biogeochemical province where productivity is limited by the micronutrient iron (de Baar et al., 1995). Regions of high productivity occur where iron is introduced into the photic zone, including at frontal zones, on shallow shelf areas around islands and continental landmasses, including Antarctica itself, and in the vicinity of zones of seasonal sea-ice coverage and polynya formation (e.g., Blain et al., 2007). Primary production in the Southern Ocean supports iconic megafauna and has enabled historic whale and seal fisheries and current fisheries, targeting krill and toothfish, to operate over the past century or more. Changes to the ecosystem structure in the Southern Ocean have the potential to cascade rapidly to higher trophic levels, altering the relative abundance and distribution of top predators (Klein et al., 2018; Reiss et al., 2017; Rogers et al., 2020; Trebilco et al., 2020). In this context, the changes in population size of krill, a key species at the base of the food web, is of major concern and led to the creation of the Convention for the Conservation of Antarctic Marine Living Resources. The combination of climate change and extractive fishery operations has resulted in Southern Ocean ecosystems that are changing rapidly such that observing and predicting anthropogenic ecosystem effects is a pressing priority.

The remote nature of the Southern Ocean makes direct observation of the marine environment and its organisms extremely challenging. Consequently, new approaches are needed to better understand spatio-temporal interactions between biogeochemical processes at the base of Southern Ocean food webs, and the distributions, movements and diets of mobile consumers. Spatial variations in the isotopic compositions of reference materials or animals can be modeled either statistically from observational data or based on mechanistic model approaches. The resulting spatial models (commonly termed "isoscapes") have been used in marine ecology to infer spatial distributions in nutrient sources that fuel primary production (Espinasse et al., 2020; MacKenzie et al., 2014), to provide isotopic baselines in trophic studies (Jennings & Warr, 2003; Pethybridge et al., 2018) and to infer animal foraging and migratory movements (Ceia et al., 2015; Cherel & Hobson, 2007; Graham et al., 2010; St. John Glew et al., 2018; Trueman et al., 2012). In this context, the development of isoscapes is relevant to a number of topics raised in a community evaluation of priority areas for research in Southern Ocean ecosystems (i.e., see the question cluster: "Antarctic life on the precipice" [Kennicutt et al., 2014]).

Spatial variations in stable carbon isotope ratios ($\delta^{13}C$) of phytoplankton are mainly driven by the isotopic composition of the dissolved inorganic carbon source and the extent of isotopic fractionation during photosynthesis, which varies among phytoplankton species and communities (Goericke & Fry, 1994; Laws et al., 1997; Lee et al., 2005; Riebesell et al., 2000). Many of the main factors influencing $\delta^{13}C$ values of photosynthesizing phytoplankton are influenced indirectly by seawater temperature (Deuser, 1970; Hofmann et al., 2000), leading to close correspondence between spatial variations of $\delta^{13}C$ values of phytoplankton and sea surface temperature (SST), especially across broad latitudinal gradients (Trueman & St John Glew, 2019). Stable nitrogen isotope values ($\delta^{15}N$) vary closely with the availability of nitrogen, primarily in the form of nitrate, and generally increase when nitrogen becomes limiting, providing information on the ecosystem primary productivity and nitrogen sources (DiFiore et al., 2010; G. H. Rau et al., 1998; Rolff, 2000). The $\delta^{15}N$ values of primary producers are also strongly influenced by the type of nitrogen available to the system, with recycled nitrogen (ammonium) and fixed N_2 gas (via diazotrophs) generating lower $\delta^{15}N$ values than new nitrate (Montoya et al., 2002; Ryabenko, 2013; Somes et al., 2010). The relatively high and sequential enrichment of ^{15}N between trophic levels also makes nitrogen isotopes useful tools in defining trophic structure in marine ecosystems (Deniro & Epstein, 1981; Hussey et al., 2014; Post, 2002).

In recent years, global scale mechanistic models have been developed for both $\delta^{13}C$ and $\delta^{15}N$, providing valuable information at broad scales to address such issues as seasonality effects and connectivity between large oceanic regions (Magozzi et al., 2017; Somes et al., 2010). In addition, the combination of statistical modeling developments and the increase in available observational data has enabled the production of observation-based isoscapes at relatively fine spatial resolutions, which have been used to resolve local scale physical and biological processes (Espinasse et al., 2020; MacKenzie et al., 2014).

In situ sample-based isoscapes have been produced for some parts of the Southern Ocean (Brault et al., 2018; Jaeger et al., 2010; Quillfeldt et al., 2010), mainly predicted for one season corresponding to the

sampling period, and developed by interpolating values between sample locations. The accuracy of interpolation-based isoscapes is dependent on the resolution and quality of the data coverage, that is, well covered areas result in meaningful interpolated data, while data from poorly resolved areas should be interpreted with caution (Brault et al., 2018). To improve isoscape accuracy, where sample collection is limited, in situ stable isotope data can be combined with measured environmental variables. By statistically modeling the relationships between measured stable isotope values and environmental data, isotope values can be predicted in regions where no isotope samples have been collected (Bowen, 2010; Bowen & Revenaugh, 2003; Espinasse et al., 2020; St. John Glew et al., 2019).

In the ocean, stable isotope values of particulate organic matter (POM) have frequently been used as a measure of processes occurring at the base of the food web (Kurle & McWhorter, 2017; Somes et al., 2010). Stable isotope values of POM have been widely collected across the Southern Ocean in the last decades for paleontology, physical, biogeochemical, and ecological research projects, producing a large number of point observations. Recent studies have highlighted the potential in applying POM stable isotope values in the Southern Ocean to produce isoscapes (Espinasse et al., 2019). In this study, we compiled POM $\delta^{13}C$ and $\delta^{15}N$ data for the Southern Ocean from unpublished and published sources and used these data to (a) build the first observation-based carbon and nitrogen isoscapes that cover the whole Southern Ocean (>40°S) and (b) quantify seasonal variations in spatial distribution of $\delta^{13}C$ and $\delta^{15}N$ values. Our principle aim here is to produce accurate isoscape models that can be used (a) in isotope-based animal movement and trophic ecology studies and (b) more generally to provide insights into the seasonality and spatial variability of large-scale ecosystem processes such as intensity of primary productivity or influence of sea-ice melting on nutrient source availability.

2. Methods

2.1. Data Collection

A meta-analysis was carried out of all published surface POM $\delta^{13}C$ and $\delta^{15}N$ data for the Southern Ocean (defined here to be south of 40°S). Isotope measurements were extracted to our database if they were georeferenced and with a known sampling date. A list of data sources including location, date, and area of sampling can be seen in Table 1.

Additional unpublished POM stable isotope data were collected during various cruises conducted in the Southern Ocean over the years 1970–2019 and were added to the data set. All published and unpublished $\delta^{13}C$ and $\delta^{15}N$ data are provided in Data Set S1. More information about the unpublished data is provided in Table S1. All water samples for unpublished POM analysis were collected either by pumping surface waters (5–10 m) onboard while underway or using sampling bottles in the upper 5 m of the water column. The POM samples were collected by vacuum filtration onto Glass Fiber Filters (GF/F) with a nominal pore size of ~0.7 μm. Most POM samples (91%) were acidified to remove carbonates before stable isotope analysis. The effect of merging acidified and nonacidified samples is taken into account in the model by including the "study" (i.e., survey) as a random factor. Similarly, carbon isotopic values were not corrected for the Suess effect (Gruber et al., 1999) as the year of sampling is also included in the model structure. A summary of sample distribution per season and per year is provided in Figure S1.

2.2. Environmental Data

We estimated that a 10-year time period was long enough to smooth interannual variability in environmental data (see e.g., the Southern Annular Mode index; Marshall, 2003). The majority of POM samples were collected during 1995–2015, and a 10-year time period of environmental data was selected between 2005 and 2015 to predict the most historically recent isoscapes as possible with the data available. Using satellite remote-sensing data, a bimonthly climatology was built for this time period, extending across the Southern Ocean from 40°S southward to the Antarctic continent, and included SST, chlorophyll-*a* (chla) concentration, net primary productivity (NPP), mixed-layer depth (MLD), sea-ice concentration, and distance from coast (Dist). Data were provided in various resolutions before being projected onto a 1° grid. A summary of data sources and value ranges can be found in Table S2. SST, MLD, and sea-ice concentration were retrieved from the Copernicus platform (marine.copernicus.eu/). SST was extracted from the Global ARMOR3D L4

Table 1
List of All Published Data Sets Containing Surface Particulate Organic Matter (POM) Carbon ($\delta^{13}C$) and Nitrogen ($\delta^{15}N$) Isotopic Data

Reference	Year samples collected	Months samples collected	Geographical area	No. of $\delta^{13}C$ measurements	No. of $\delta^{15}N$ measurements
Eadie and Jeffrey (1973)	1970	Dec	Indian sector	3	NA
Wada et al. (1987)	1983–1984	Dec–Jan	South of Australia	2	2
G. Rau et al. (1991)	1986	Mar	Atlantic sector	28	NA
Altabet and Francois (1994)	1991	Feb	Indian sector	46	46
Francois et al. (1993)	1991	Feb	Indian sector	48	NA
Dehairs et al. (1997)	1991–1992	Oct–Jan	Atlantic/Pacific sectors	44	NA
Bentaleb et al. (1998)	1992	Mar	Indian sector	43	NA
Kennedy and Robertson (1995)	1992	Dec	Pacific sector	51	NA
Riaux-Gobin et al. (2006)	1993	Apr	Indian sector	12	NA
Popp et al. (1999)	1994	Jan	Indian Ocean/South of Australia	56	NA
Trull and Armand (2001)	1994–1996	Jan, Jul, Sep, and Nov	South of Australia	198	NA
O'Leary et al. (2001)	1995	Nov	South of Australia	24	NA
Lourey et al. (2003, 2004)	1997–1998	Dec–Mar, Sep, and Nov	South of Australia	169	140
Schmidt et al. (2003)	1999–2000	Mar–Apr	Atlantic sector	4	4
Espinasse et al. (2019)	2004–2006	Apr–May, Nov–Jan, and Jun–Jul	Atlantic sector	225	218
Lara et al. (2010)	2005	Mar–Apr	Argentine shelf-Antarctic peninsula	69	69
Zhang et al. (2014)	2006	Jan	Indian sector	24	NA
Richoux and Froneman (2009)	2007	Apr	Indian sector	2	2
Barrera et al. (2017)	2012	Apr	Drake passage	3	3
Montecinos et al. (2016)	2013	Apr	Pacific sector	2	2
Horii et al. (2018)	2014	Jan	Pacific sector	1	1
Giménez et al. (2018)	2014	Feb	Argentine shelf	3	3
Seyboth et al. (2018)	2013–2016	Nov–Mar	Antarctic Peninsula	115	112

Reprocessed data set, which provides high-resolution temperature and salinity fields derived from in situ and satellite observations (Guinehut et al., 2012). MLD and sea-ice concentration were issued from the GLORYS12V1 product, which is a global ocean eddy-resolving reanalysis covering the satellite altimetry era 1993–2018 (more information can be found on the Copernicus platform). Chla concentrations were collected from GlobColour (http://globcolour.info/). GlobColour delivers a merged product that uses all satellite data available at the processing time (Maritorena et al., 2010). Different models have been developed to produce NPP based on chla concentrations and incident irradiance. It is difficult to reconcile which of these models provides data that are closer to in situ observations due to the lack of validation in the Southern Ocean (Strutton et al., 2012). We estimated NPP using the Eppley Vertically Generalized Production Model (Eppley-VGPM) calculation. The Eppley-VGPM calculation is an adaptation of the VGPM approach (Behrenfeld & Falkowski, 1997), in which the polynomial description of light-saturated photosynthetic efficiencies as a function of SST is replaced with the exponential relationship described by Morel (1991) and based on the curvature of the temperature-dependent growth function described by Eppley (1972). The code to run the Eppley-VGPM calculation was acquired from Oregon State University (science.oregonstate.edu/ocean.productivity/). The calculation of the NPP used SST, chla, and photosynthetically active radiation data (obtained from GlobColour) as inputs. Chla and NPP products are dependent on atmospheric conditions, resulting in missing data for some areas due to persistent cloud coverage. The distance to the coast was calculated as distance from the center point of the grid cell to the 500 m isobath.

While the climatology was originally produced at bimonthly resolution, the six austral winter months (May–October) were further merged together as few data were available for this timeframe, and during this period the system is less dynamic due to low light conditions (Arteaga et al., 2020). In addition to the

Table 2
Best Fit (No-Interaction and First-Order Interaction) Models for Surface Particulate Organic Matter (POM) Carbon ($\delta^{13}C$) and Nitrogen ($\delta^{15}N$) Isotope Values With Environmental Covariates (SST = Sea Surface Temperature, Dist = Distance From Land, NPP = Net Primary Productivity, and MLD = Mixed-Layer Depth) and Fixed Effects of Year and Season (January/February, March/April, May–October, and November/December), With Associated Deviance Information Criteria (DIC) Values and Correlation Coefficients of Predicted Values Against Measured Values

Model	DIC	Correlation coefficient	Random effects precision (mean (credible intervals))		
			Season	Year	Study ID
$\delta^{13}C \sim -25.8 + 2.28 \times SST + 0.27 \times NPP + 0.01 \times MLD + f(Year) + f(Season) + f(Study)$	12,818	0.86	11.5 (2.3, 32.5)	0.9 (0.5, 1.4)	0.4 (0.2, 0.7)
$\delta^{13}C \sim -26.2 + 2.82 \times SST - 0.51 \times NPP - 0.22 \times MLD - 0.68 \times Dist - 0.42 \times SST:NPP - 0.34 \times MLD:NPP - 0.76 \times Dist:NPP + f(Year) + f(Season) + f(Study)$	12,646	0.86	4.5 (1.0, 12.8)	1.5 (0.9, 2.2)	0.5 (0.3, 0.7)
$\delta^{15}N \sim 0.09 + 0.89 \times NPP - 0.88 \times MLD - 0.46 \times Dist + 0.4 \times SST + f(Year) + f(Season) + f(Study)$	12,644	0.87	16.6 (1.2, 86.1)	2.8 (1.2, 6.0)	0.9 (0.4, 1.8)
$\delta^{15}N \sim -0.07 + 1.19 \times NPP - 0.26 \times MLD - 0.49 \times Dist + 0.27 \times SST + 0.4 \times SST:NPP + 0.79 \times MLD:Dist + 0.7 \times MLD:NPP + f(Year) + f(Season) + f(Study)$	11,072	0.76	5.9 (5.3, $5.3e^5$)	2.0 (1.1, 3.7)	0.7 (0.2,1.5)

Note. The precision (precision = 1/variance) mean and credible interval for each random effect term are also stated.

seasonal values, a yearly average was calculated. Each environmental covariate value (yearly average and seasonal value) was extracted at each POM sampling location and scaled by subtracting the variable mean from each value and dividing by the variable standard deviation.

2.3. Isoscape Modeling

Isoscapes predicting $\delta^{13}C$ and $\delta^{15}N$ values across the Southern Ocean were modeled using a Bayesian hierarchical spatial modeling framework, Integrated Nested Laplace Approximation (INLA), via the R-INLA package (http://www.r-inla.org/; Rue et al., 2009). This approach was adopted to enable uncertainty due to spatial variability in sample collection seasons and year to be estimated. For a full description of the benefits of the INLA approach in marine isoscape modeling, refer to St. John Glew et al. (2019). Values of $\delta^{13}C$ and $\delta^{15}N$ were modeled as a function of a set of environmental covariates $\boldsymbol{X}_i$, with year, season, study, and the underlying spatial effect included as random effects. Models were specified as

$$Y_i \sim \text{Intercept} + \boldsymbol{\beta}_i \boldsymbol{X}_i + f(T_i) + f(U_i) + f(V_i) + f(W_i) + \varepsilon_i$$

$$T_i \sim \text{N}(\text{O}, \sigma^2_{\text{season}})$$

$$U_i \sim \text{N}(\text{O}, \sigma^2_{\text{year}})$$

$$V_i \sim \text{N}(\text{O}, \sigma^2_{\text{study}})$$

$$W_i \sim \text{N}(\text{O}, \Omega)$$

$$\varepsilon_i \sim \text{N}(\text{O}, \sigma^2) \quad (1)$$

where Y_i is the isotope value ($\delta^{13}C$, $\delta^{15}N$) at location i; $\boldsymbol{X}_i$ is a vector containing the environmental covariates as linear fixed effects; $\boldsymbol{\beta}_i$ is a vector of parameters to be estimated; T_i, U_i, and V_i are the season, year, and study random effects, respectively, with assumed Gaussian distributions; W_i represents the smooth spatial effect, linking each observation with a spatial location, with the elements of the spatial domain Ω estimated using the Matérn correlation; and ε_i contains the independently distributed residuals. All individual POM data were included in the model, including locations where multiple samples were collected at the same location.

Environmental variables to be used in the model (Figure S2) were first selected by performing covariance tests and removing covarying variables with the weakest correlation to both $\delta^{13}C$ and $\delta^{15}N$ values. Sea-ice cover and chla concentration were thus removed from further analysis.

Model selection was based on deviance information criteria and model fit (Pearson's correlation coefficient between predicted and observed values) and was determined by manually running different combinations of covariates and removing the least important covariates in a stepwise process, beginning with the full global model containing all covariates (SST, MLD, PPT, and Dist). More details about the model selection process can be found in Text S1. Twelve-month average environmental variables were used for model selection.

Best fit models were derived containing both no-interaction terms and first-order interaction terms (Table 2). Models excluding interaction terms are likely to be more useful for interpreting the most important covariates influencing isotopic variability over larger spatial scales, whereas models containing first-order interaction terms are likely to be able to incorporate

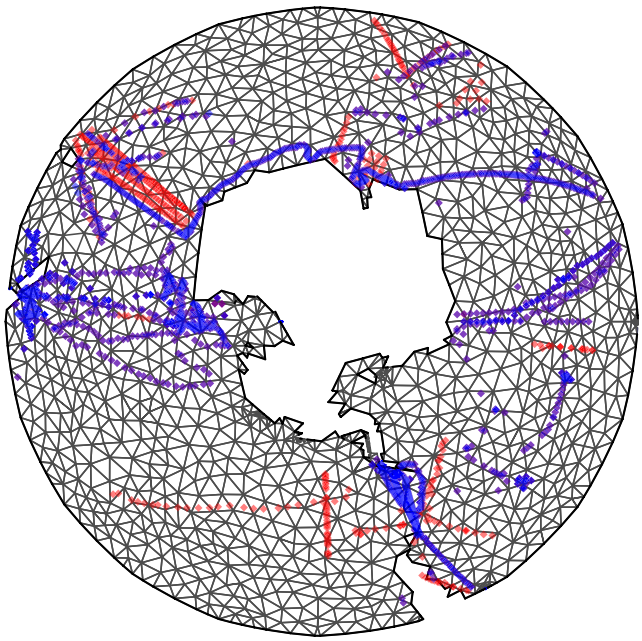

Figure 1. Delaunay triangulation mesh for the Southern Ocean: carbon data points = red, nitrogen = blue. Where both carbon and nitrogen data were available points may appear purple.

smaller scale local variability and predict more precise isoscape models (St. John Glew et al., 2019). Noninformative default priors were used for each model.

The best fit models (both including and excluding interaction terms) were used to predict $\delta^{13}C$ and $\delta^{15}N$ values in POM across the whole Southern Ocean spatial domain using continuous raster surfaces of 12-month averaged, scaled environmental variables as predictors. To ensure that predicted values fell within a sensible range, environmental variable surfaces were assessed to check that all values used for predictions fell within the range of values observed at POM sampling locations. The majority of environmental variable surface values fell within the observed location range, but any outlier grid cells were clipped from the raster surfaces. Response variables were estimated at all mesh vertices (Figure 1), which were then linearly interpolated within each triangle into a finer regular grid (2° × 1°) via Bayesian kriging. Mesh maximum edge (triangle size) was selected using a sensitivity analysis, by selecting the smallest triangle size which notably increased model performance, while also accounting for computing time. Mean and variance predictions were obtained for each grid cell. Predictions were mapped to produce carbon and nitrogen isoscapes and model variance surfaces representing expected average isotopic compositions for POM across the Southern Ocean when accounting for variability in sample collection year and season. All models were mapped on a polar projection EPSG 3031 (WDG 84, Antarctic Polar Stereographic).

2.4. Seasonal Differences

Four different methods were explored to model the seasonal carbon and nitrogen isotopic differences within the Southern Ocean (Text S2 for method details and Figure S3 for isoscapes). Eventually, models including the universal covariate terms (model described in Section 2.3), but excluding season, were run on season-specific isotopic data enabling the coefficient terms to vary between seasons. These season-adjusted models were then used to predict seasonal isoscapes by applying season-specific environmental data. Predicted isoscape surfaces for March–April (autumn), May–October (winter), and November–December (spring) were then subtracted from the January–February (summer) isoscapes (the season with the highest number of data points) for both carbon and nitrogen (no-interaction and interaction model predictions) to demonstrate seasonal variability in $\delta^{13}C$ and $\delta^{15}N$ values across space. Details of the best fit models can be seen in Table S3.

3. Results

3.1. POM Data

In total, 3,237 carbon and 2,614 nitrogen POM data points were compiled from across the Southern Ocean at 2,766 and 2,215 locations, respectively (Figure 2). Data were collected across 31 different years from 1970 to 2019, with most data collected from 1995 to 2015. Data were collected across all seasons, with most samples collected in January–February during the austral summer (Figure 2). No strong spatial bias in sample collection season was observed, with many regions sampled across multiple seasons (Figure 2). The $\delta^{13}C$ and $\delta^{15}N$ value ranges of all POM samples were −36.84‰ to −16.49‰ and −6.09‰ to +10.80‰, respectively.

3.2. Southern Ocean Isoscape Models

The best fit carbon and nitrogen prediction models, both excluding and including first-order interaction terms, are displayed in Table 2. The strongest covariate predictors for $\delta^{13}C$ variability were SST, NPP, and MLD. The same covariates, with the addition of distance from land, were significant predictors for $\delta^{15}N$

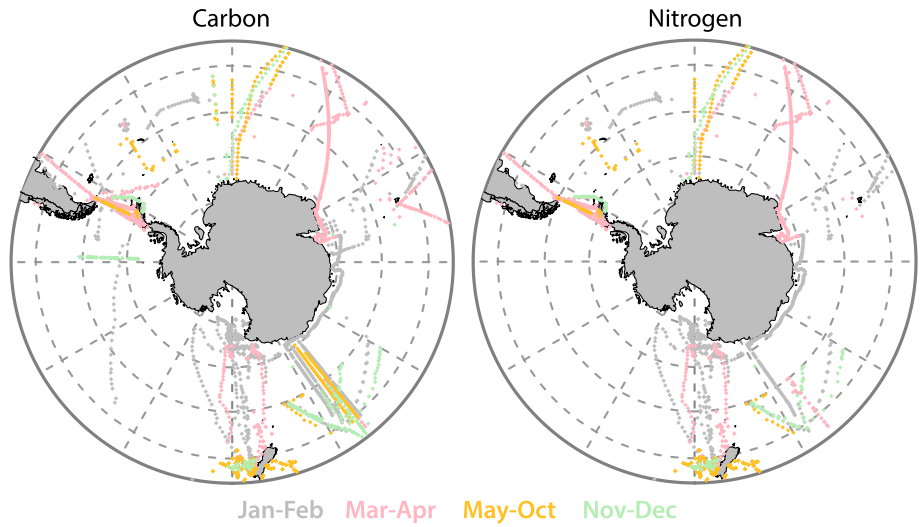

Figure 2. Locations of surface particulate organic matter (POM) samples for carbon ($\delta^{13}C$) and nitrogen ($\delta^{15}N$) isotope analysis, collected across the Southern Ocean in January–February (gray), March–April (pink), May–October (yellow), and November–December (green).

variability. The best fit models were able to explain 86% and 74%–76% (correlation coefficient) of the spatial variability observed in carbon and nitrogen isotopes, respectively (Table 2).

Spatial distributions of $\delta^{13}C$ data across the Southern Ocean are largely consistent with previous research showing relatively low $\delta^{13}C$ values at higher latitudes (−31‰ to −28‰) and gradually increasing with distance from the polar region to values of −24‰ to −20‰ at 40°S (Figure 3). Higher $\delta^{13}C$ values are also predicted closer to land (−22‰ to −19‰), both east and west of southern South America and New Zealand. Spatial distributions of $\delta^{15}N$ across the Southern Ocean varied between sectors, with relatively negative $\delta^{15}N$ values observed in the Pacific Ocean sector (−6‰ to −1‰), compared to slightly more positive values observed in the Atlantic (−1‰ to 4‰) and Indian ocean sectors (−2‰ to 1‰). Notably higher $\delta^{15}N$ values (3‰–10‰) were predicted in the vicinity of land masses, both east and west of southern South America, around New Zealand, and south of Tasmania (Figure 3).

Variance surfaces show broadly similar patterns for both carbon and nitrogen models, with less than 0.4‰ uncertainty values across the majority of the Southern Ocean (Figure 3). For both carbon and nitrogen isoscapes, predictions based on the models including first-order interactions increased the predicted isotopic range and spatial differences at more local resolutions. Introduction of interaction terms also increased uncertainty values from less than 0.4‰ up to approximately 1‰ in certain regions, such as within waters leading to the Pacific Ocean and Indian Ocean, where in situ data samples are scarce (Figure 3).

3.3. Seasonal Differences

Similar residual isotopic variability between seasons was observed in all $\delta^{13}C$ and $\delta^{15}N$ models, with approximately 1‰ difference between seasons not accounted for by the variables in the selected models (Figure S4). Within the $\delta^{13}C$ models, isotopic differences occurring during the January and February summer months were most different to the remainder of the year, with positive residual values in comparison to the winter months (May–October). Within the $\delta^{15}N$ models, isotopic residual values were most different in spring (November–December), with higher unexplained values compared to the rest of the year.

Carbon isotope values were predicted to vary between season by approximately ±4‰ on average, but up to ±8‰ in certain regions (Figure 4). In the most northerly regions of the Southern Ocean, the highest $\delta^{13}C$ values were predicted in both carbon models during the summer months of January and February. In the more southerly regions, surrounding Antarctica, the highest values were predicted in March and April, with the lowest $\delta^{13}C$ values predicted in peak summer months. Overall, the lowest $\delta^{13}C$ values were predicted in winter months (May–October), particularly within the Pacific Ocean (Figure 4).

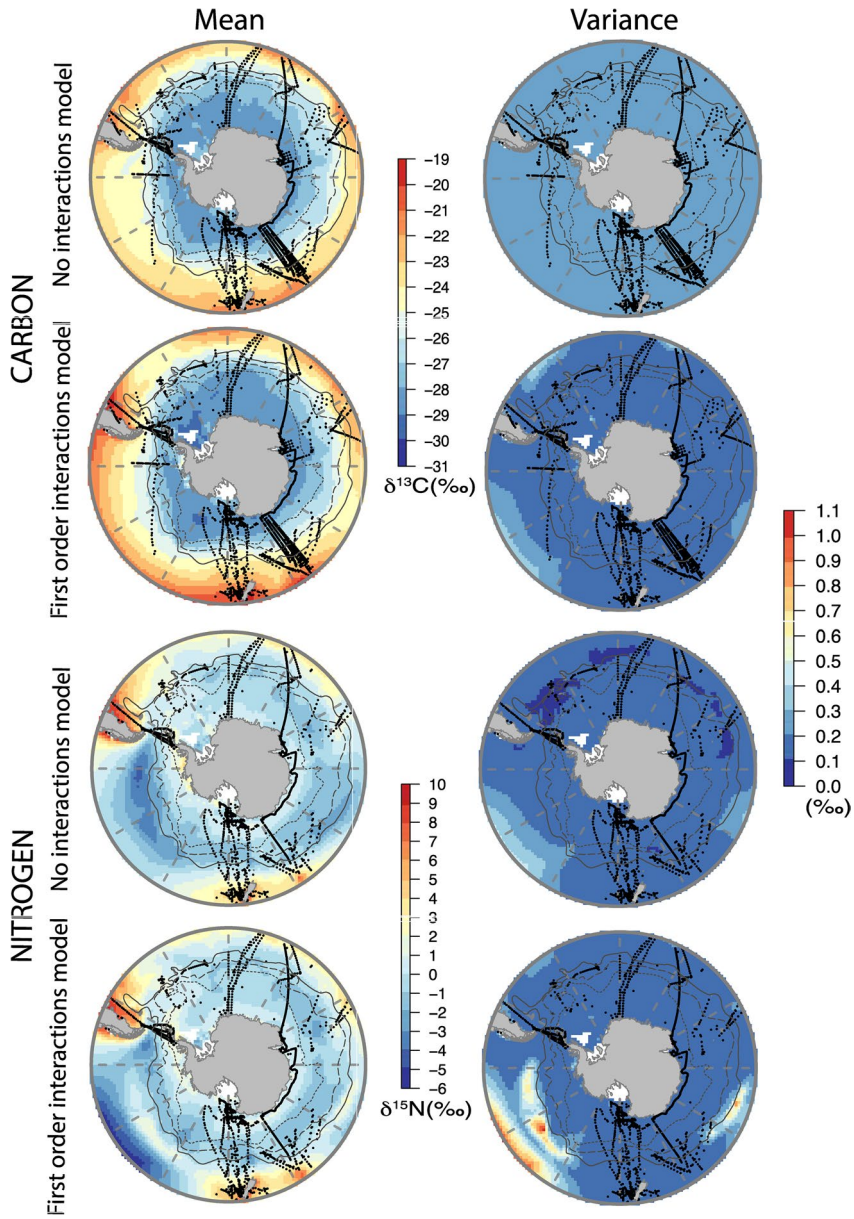

Figure 3. Southern Ocean surface particulate organic matter (POM) carbon ($\delta^{13}C$) and nitrogen ($\delta^{15}N$) 12-month average isoscape predictions, derived from models both excluding and including interaction terms, and the associated variance of the posterior predicted distribution, after seasonal and yearly random effects have been accounted for. Black dots represent sample locations. Paths of the Southern Ocean fronts are shown in dark gray (solid line: Sub-Antarctic Front; dashed line: Polar Front; and dotted line: southern Antarctic Circumpolar Current Front as described by Orsi and Harris [2019]).

Nitrogen isotope values were predicted to vary between seasons more than carbon isotope values, with average isotopic differences of ±4‰, but with differences of up to ±16‰ occurring in some regions, such as the open ocean regions of the Pacific and Indian sectors and east of Argentina (Figure 5). The highest $\delta^{15}N$ values were predicted in spring (November–December) across the majority of the Southern Ocean. An exception was the area east of Argentina, where the highest $\delta^{15}N$ values were predicted to occur in summer (January–February). Nitrogen isotope values were predicted to be relatively low during the autumn months (March–April) across the majority of the Southern Ocean. Values of $\delta^{15}N$ were predicted to be rather variable in winter months, exhibiting values that may be either lower or higher than those predicted for summer months. The two model types also predicted different patterns, with extremely low $\delta^{15}N$ values (−16‰

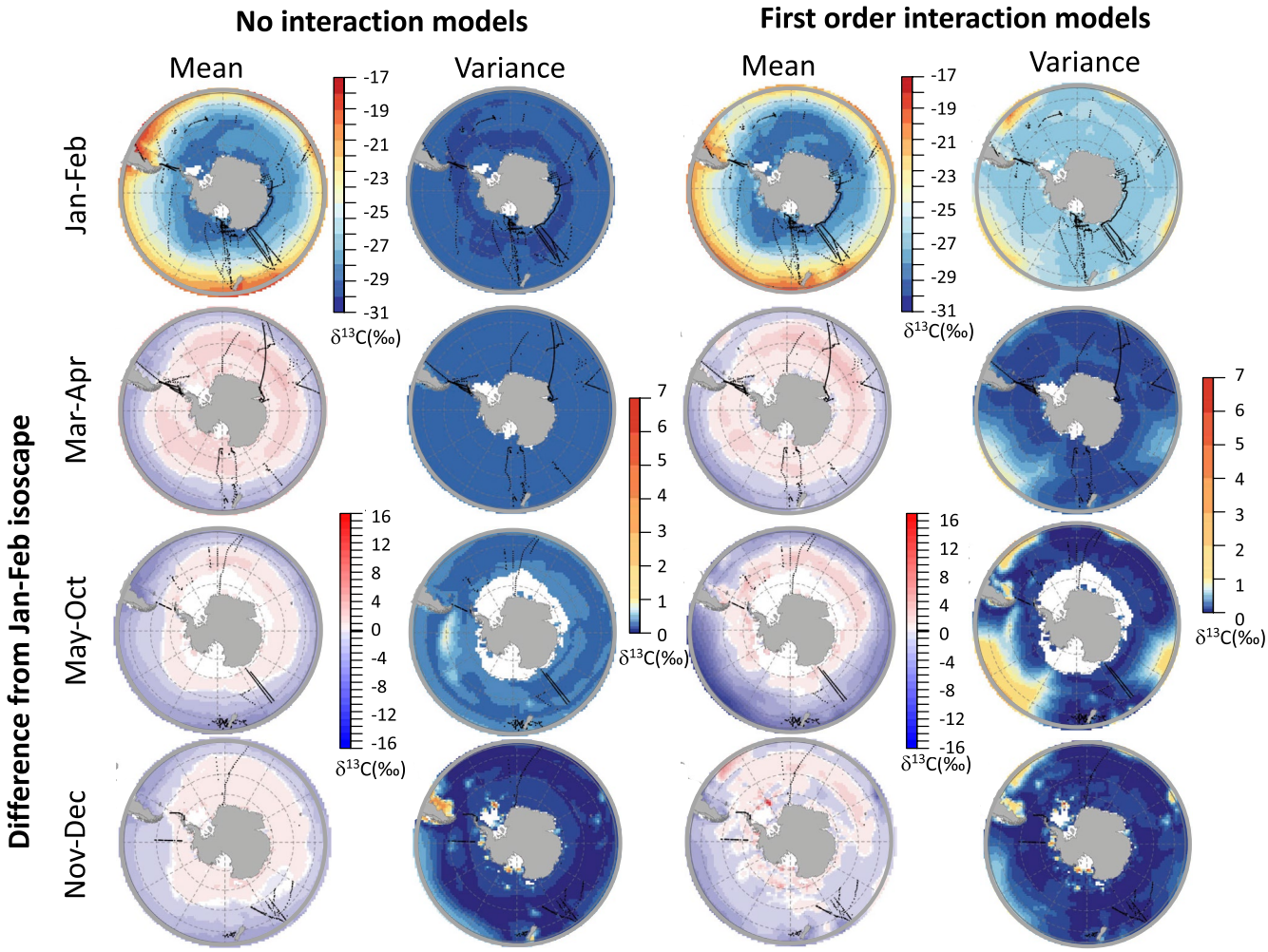

Figure 4. January–February summer season-specific carbon ($\delta^{13}C$) no-interaction term and first-order interaction term isoscape prediction. The spatial isotopic differences of each season compared to the January–February prediction (each season prediction minus January–February prediction) are also shown. Blue areas depict regions which are predicted to have lower carbon isotope values compared to January and February, and red areas depict regions which are predicted to have higher $\delta^{13}C$ values during that season. Variance surfaces for each seasonal model prediction are also shown. Data points are shown as black dots.

to −2‰) predicted in the open ocean areas in the no-interaction models, but extremely high $\delta^{15}N$ values (8‰–16‰) predicted in the first-order interaction model (Figure 5).

Isoscape model variance values for carbon in all seasons and for nitrogen in January–February and March–April were relatively low with values in most areas being less than 2‰. There was increased variance for both carbon and nitrogen within the open ocean areas of the Pacific and Indian Oceans where limited data were collected. The highest carbon and nitrogen variance values were observed in the winter (May–October) isoscape predictions where fewer POM samples were collected compared to all other seasons. First-order interaction models had greater variance values than the no-interaction models.

4. Discussion

This study provides a significant improvement in the prediction of carbon and nitrogen isoscapes across the Southern Ocean, in comparison to previously produced global mechanistic model predictions (Magozzi et al., 2017; Somes et al., 2010; see Figure S5) and regional scale sample-based predictions (Brault et al., 2018; Jaeger et al., 2010; Quillfeldt et al., 2010). The yearly modeled $\delta^{13}C$ values were strongly driven by temperature, decreasing toward the pole, following the expected gradient of increasingly more negative

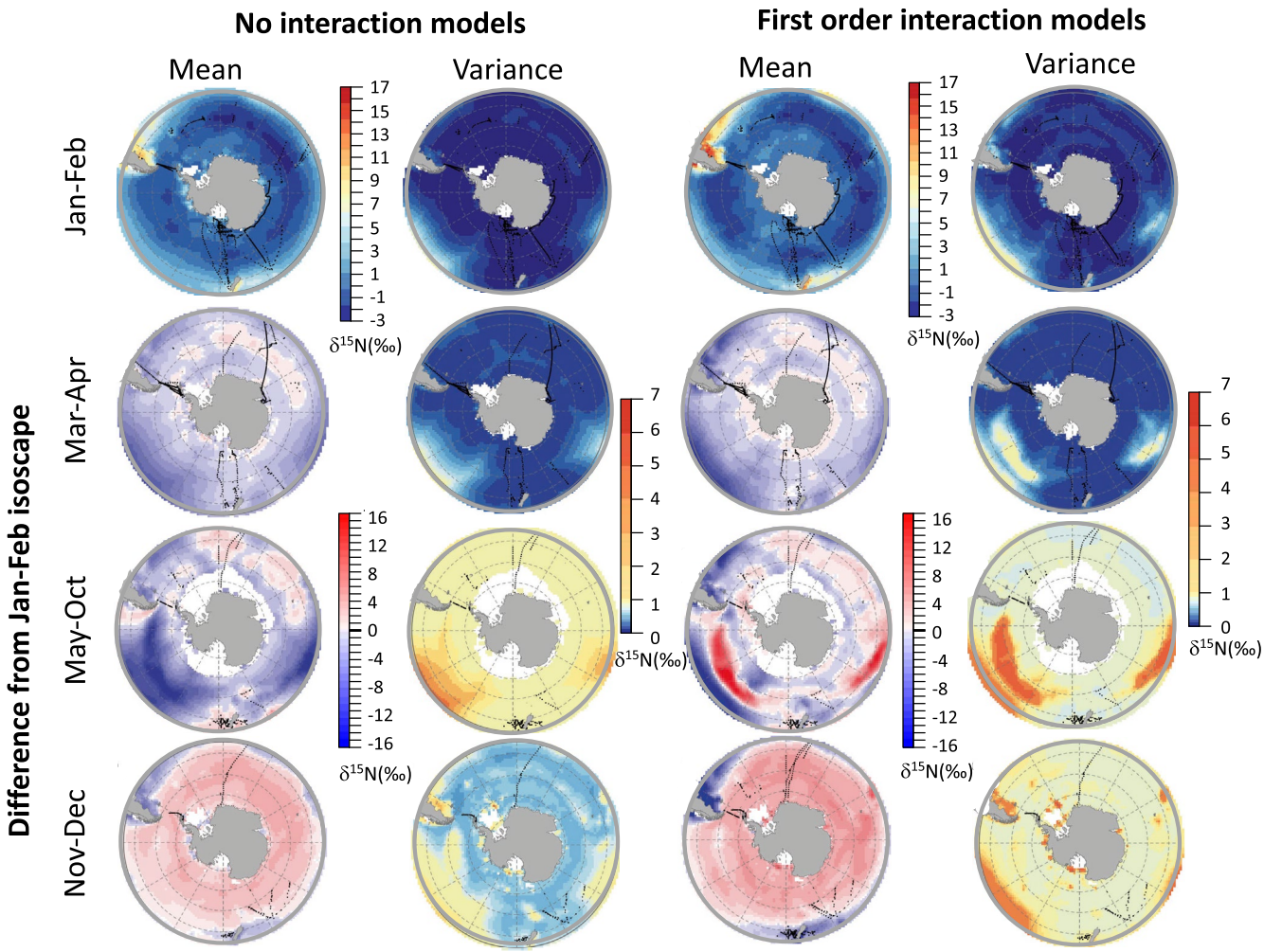

Figure 5. January–February season-specific nitrogen no-interaction term and first-order interaction term isoscape prediction. The spatial isotopic differences of each season compared to the January–February prediction (each season prediction minus January–February prediction) are also shown. Blue areas depict regions which are predicted to have lower nitrogen isotope values compared to January and February, and red areas depict regions which are predicted to be higher in $\delta^{15}N$ during that season. Variance surfaces for each seasonal model prediction are also shown. Data points are shown as black dots.

isotopic values toward the polar latitudes (Goericke & Fry, 1994; Quillfeldt et al., 2010; G. Rau et al., 1991). Changes across longitude mainly tracked North/South variations in the position of the Polar Front. Elevated $\delta^{15}N$ values coincided with areas of higher primary production, generally located down-current (east) of land masses or islands or above shallow shelves that extend around the continents and islands of the Southern Ocean.

Seasonal modeled carbon and nitrogen isoscapes had higher variability in predicted values than the 12-month averaged isoscapes, particularly for winter/spring months, which were commonly under sampled. Values of $\delta^{13}C$ were largely driven by surface ocean temperatures, with higher $\delta^{13}C$ values predicted earlier in the seasonal cycle at lower latitudes, where temperatures were warmer. Maximum $\delta^{13}C$ values in January–February were predicted north of the Polar Front, but March–April maximum values occurred to the south. Nitrogen isotope values peaked in November–December (spring), corresponding to high pelagic production at low latitudes, coinciding with the release of nutrient-enriched water from sea-ice melt at high latitudes.

4.1. $\delta^{13}C$ Spatial and Seasonal Variability

As expected, SST, as the driver for CO_2 concentration in seawater, was the predominant factor explaining geographic and seasonal changes in $\delta^{13}C$ values in our model, with a large range of measured SST values and predicted $\delta^{13}C$ values from 40°S to the Antarctic continent. The second key predictor of $\delta^{13}C$ variability was NPP. While both primary productivity and chla concentrations from satellites were considered as potential predictors early in the modeling process, primary productivity emerged to be a more powerful predictor during the parameter selection process. The approach for estimating primary productivity took into account several parameters such as irradiance and temperature and also includes a temperature-dependent description of photosynthetic efficiencies (Behrenfeld & Falkowski, 1997). The amount of light in the Southern Ocean varies significantly with latitude, and also MLD, and this will affect photosynthetic efficiency (Bracher et al., 1999). By taking into account latitudinal changes in daily irradiance and temperature, primary productivity estimates might better correlate with seasonal and spatial variations in phytoplankton development, which in turn affect carbon uptake and thus $\delta^{13}C$ values over the wide latitudinal range covered in this study.

The predicted $\delta^{13}C$ values presented in this study are comparable to the values modeled by Magozzi et al. (2017). Both carbon isoscapes predicted a similar range of values (−20‰ to −30‰) with higher values at low latitudes such as around the continental shelves of South America and Tasmania/New Zealand and lower values found within the Weddell and Ross Seas (Figure 3). Overall, the Magozzi et al. (2017) model predicted lower $\delta^{13}C$ values with a median offset of 2‰. Including first-order interactions, our INLA model produced a better match between statistical and mechanistic isoscape models, with interaction terms removing extreme $\delta^{13}C$ values predicted east and west of South America. Including first-order interaction terms reduced the standard deviation of the offset between statistical and mechanistic isoscape models from 1.2‰ to just 0.6‰ (Figure S6). The estimated interseasonal variability was also comparable with a range of 6‰ at 60°S modeled by Magozzi et al. (2017) and seasonal anomalies mainly between −4‰ and 4‰ in the present study (Figure 4). However, we observed a slight temporal offset in peak $\delta^{13}C$ value timings: at location 60°S/−90°E, with maximum values predicted in January–February by Magozzi et al. (2017) compared to March–April in our study. In general, south of the Polar Front, $\delta^{13}C$ values were relatively stable between seasons, most likely due to limited variation in water temperatures within this region. The model did not fully depict the high variability in $\delta^{13}C$ values sometimes observed in this area (Munro et al., 2010). High variability can be due to the release of brine waters from ice melting, which are enriched in ^{13}C (Munro et al., 2010), and promote phytoplankton development due to increased iron input (Lannuzel et al., 2016). North of the Polar Front, highest $\delta^{13}C$ values were predicted in summer (January–February), in agreement with the temperature cycle in this region. Very low values were predicted in the Pacific Ocean during winter, although these values were associated with high uncertainties and should therefore be taken with caution. Another noteworthy feature was that the $\delta^{13}C$ values on the Patagonian shelf were predicted to peak early in the year, potentially as a result of the phytoplankton bloom happening in October (considered in this study as a winter month; Carreto et al., 2016), earlier than in other areas at a similar latitude. Intense phytoplankton blooms can lead to increased $\delta^{13}C$ values by locally decreasing the concentration of aqueous CO_2 (Deuser, 1970). It should be noted, however, that these values were also associated with high uncertainties and should be interpreted with caution.

4.2. $\delta^{15}N$ Spatial and Seasonal Variability

Primary productivity and MLD were the two main factors driving $\delta^{15}N$ variability in our model. Both are important processes in controlling the concentration and availability of nitrogen-based nutrients in the euphotic layer. Phytoplankton uptake of nutrients for growth will diminish the nutrient pool, while wind mixing and high energetics of the ACC (Sokolov & Rintoul, 2009) will replenish the nutrient pool by mixing deep, nutrient-rich water into the surface layer. The degree of mixing is positively correlated with MLD, although it is not necessarily true at small time scales (Franks, 2015). Nitrate concentrations in the Southern Ocean are generally higher south of the Polar Front and decrease north of the Polar Front (Switzer et al., 2003) where primary productivity is on average greater. The MLD was highest in the open ocean zone south of the Polar Front. This allows for euphotic zone nitrate replenishment but the deep MLD can also

result in light limitation of phytoplankton growth (Deppeler & Davidson, 2017). The MLD gets shallower south of the southern Antarctic Circumpolar Current Front, especially in the MIZ during sea-ice melt.

The two other factors playing a role in $\delta^{15}N$ variability were distance to land and SST. Coastal environments are usually characterized by higher carbon and nitrogen stable isotope values that decrease with distance offshore (Kline, 2009; Lara et al., 2010; Zhang et al., 2014). The drop in $\delta^{13}C$ values is usually sharp, occurring in the near coastal area, but $\delta^{15}N$ values can remain high over tens to a few hundred kilometers from the coast (El-Sabaawi et al., 2012). The spread of this coastal signal depends not only on surface water advection and mixing but also on coastal-sourced iron concentration, which can sustain new production until exhaustion (Blain et al., 2007; Bucciarelli et al., 2001; Mongin et al., 2008). A potential explanation is that ^{12}C within surface waters is able to be readily replenished by atmospheric exchange, while replenishment of ^{14}N within surface waters is mostly dependent on mixing with deeper waters and, therefore, is dependent on mixing conditions. This may potentially explain why distance to coast is a significant predictor in the nitrogen model, but not in the carbon model. SST likely plays an indirect role in $\delta^{15}N$ variation, by acting as a proxy for the latitudinal increase of nutrient availability from north to south (Switzer et al., 2003).

The combination of the four principle factors (NPP, MLD, SST, and Dist) result in the delineation of two distinctly different biogeochemical regimes, north and south of the Polar Front. North of the Polar Front, $\delta^{15}N$ values varied closely with the intensity of primary production as the lower starting levels of nitrate are more prone to depletion and correspondingly, an increase in phytoplankton $\delta^{15}N$ values. South of the Polar Front, $\delta^{15}N$ values are low in the open ocean but increase in the MIZ where meltwater can result in shallower MLDs constraining nutrient-rich waters in the photic zone. The release of micronutrient such as iron promotes phytoplankton growth and associated nitrates uptake (Lannuzel et al., 2016; Tagliabue et al., 2017). Sea-ice concentration, although thought to be an important factor, was removed from the model due to a strong correlation with SST. Sea-ice concentration may be a stronger predictor of $\delta^{15}N$ values if just focusing on the region south of the Polar Front, however, for the whole Southern Ocean, SST was proven to be a more powerful predictor.

It is notoriously difficult to model nitrogen isoscapes based on a mechanistic approach. Somes et al. (2010) were the first to do so at a global scale, predicting $\delta^{15}N$ values varying between 0‰ and 6‰ south of 40°S, which is a narrower range than predicted here (−2‰ to 8‰; Figure S6). Offsets between statistical and mechanistic nitrogen isoscapes varied over a large 15‰ range, highlighting the complexity of nitrogen isotope dynamics. In general, statistical interpolation models predicted higher $\delta^{15}N$ values than mechanistic models at the margins of the Antarctic continent, around the Patagonian shelf and Scotia Arc. This is potentially due to increased predictive precision within highly productive areas where the uptake of nitrate results in high $\delta^{15}N$ values that may not be captured in the mechanistic model. By contrast, the mechanistic model predicted higher $\delta^{15}N$ values than statistical observation at higher latitudes. In contrast to the Somes et al. (2010) nitrogen isotope model, INLA models that allow first-order interactions produced greater variance between statistical and mechanistic nitrogen isoscapes (standard deviation of offset values: 2.6‰ for no-interaction model and 3.25‰ for the interaction model).

The modeled seasonal changes in $\delta^{15}N$ values should be considered carefully because models suggested high uncertainties for winter (May–October) and spring (November–December; Figure 5). Seasonal isoscape predictions showed higher $\delta^{15}N$ values occurring in November–December for a large part of the Southern Ocean, excluding productive areas over continental shelves. Even though the Southern Ocean is a HNLC region, where phytoplankton development is mainly limited by iron inputs (Boyd et al., 2000; Martin, 1990; Trull & Armand, 2001), the decrease of the nitrate pool during the spring bloom is followed by an increase in $\delta^{15}N$ values in POM (DiFiore et al., 2010). Furthermore, the melting of the sea ice is associated with a release of sea biota (phyto- and microzooplankton), which are enriched in ^{15}N (Fripiat et al., 2014). As this process is not directly translated into the model (Table 2), it could be the cause of higher $\delta^{15}N$ values, which are unexplained by the model for spring (November–December; Figure S4).

4.3. Model Structure

In this investigation, two different statistical isoscape models were built and presented: (a) including or (b) excluding first-order interactions terms between environmental predictor variables in the model structure.

Including interaction terms not only enabled a larger range of isotope predictions and associated variance to be captured but also complicates the model structure and therefore interpretation of the outputs. The simpler, no-interaction term models allowed for manageable interpretation of model relationships between the covariate and dependent variables, which could then be aligned to known ecological processes, as discussed above. Simple, no-interaction term isoscapes are useful for comparing broad-scale differences in isotopic ratios across space and for studies describing the underlying physical and biogeochemical mechanisms responsible for spatiotemporal variations in stable isotope values. Models including interaction terms explain more of the variance observed in data and therefore produced more precise and potentially more accurate spatial isotopic predictions. Accurate and precise isoscapes are particularly valuable for animal geolocation studies (Cherel & Hobson, 2007; Trueman & St John Glew, 2019), especially when identifying the organism's origin using relatively fast turnover tissues (blood plasma, muscles; Jaeger et al., 2010) or piecing together migration history by performing high-resolution sampling of calcified tissues (e.g., otoliths; Darnaude & Hunter, 2018; Sakamoto et al., 2019; Trueman et al., 2012). The underlying spatial structure in the isoscape model uncertainty (variance isoscapes) is also critical for animal assignment studies, highlighting the regions where isoscape predictions are less accurate either due to limited data availability, locally high variance in predictor variables, or predictor values in the projected region which are out of the range of those in the observed areas. Spurious prediction can also be the result of a combination of limited data and strong influential interaction. For example, within the Pacific Ocean, winter predictions of high $\delta^{15}N$ POM values are related to deep MLD (>300 m depth) and low primary productivity but are hard to relate to ecological processes. Assuming that uncertainty terms are included in an assignment process, it will always be more difficult to assign an individual or population of individuals to a region where the isoscape prediction has higher uncertainty, even if the isotope values of the isoscape and assignment animal tissue are a close match (Wunder, 2010).

The results presented here highlight the need for baseline seasonal isotopic variability to be accounted for when using isoscapes for animal assignment purposes. In the present study, both carbon and nitrogen values varied significantly within the same geographic location between seasons, with variations of up to approximately 10‰ for nitrogen and 4‰ for carbon. The strength of isotopic differences between geographic regions within the Southern Ocean was also seen to vary between seasons, with key implications for the ability to assign an animal to its origin during different seasons. High levels of seasonal variance in isoscapes could potentially improve the potential to assign an animal to a location within an isotopically differentiated area but reduce the ability to assign an animal to an area in more homogenous months. In any case, knowing the extent and spatial expression of seasonal variation in isoscapes is critical for accurate reconstruction of trophospatial ecology (Trueman et al., 2019). Diet assimilation is also likely to be highly seasonal for higher trophic level organisms, and ideally season-specific isoscapes should be utilized in regions with strong indications for seasonal variability. However, as this is likely not possible in many scenarios, we propose the weighting of mean annual isoscapes by seasonal production to incorporate intra-annual variability.

4.4. Using POM to Construct Stable Isotope Baselines

POM stable isotope data were used to build the isoscapes presented here, although it should be noted that the suitability of POM as a reference for construction of isoscape models has been widely debated. POM composition and isotopic values can be highly variable in time depending on factors such as nutrient sources (Lara et al., 2010; Stowasser et al., 2012), water column stratification (O'Leary et al., 2001; Zhang et al., 2014), the intensity of primary production (Stowasser et al., 2012), plankton community composition, physiology and growth rates (O'Leary et al., 2001; Trull & Armand, 2001), and microbial and grazing activity (O'Leary et al., 2001). The temporal dynamics of these processes can result in a fast turnover rate and high local variability. Therefore, it has been questioned whether POM provides a suitable baseline over large areas and over medium- to long-term time scales, which are all requirements in animal tracking studies, for example. There is a practical reason why POM was used to develop isoscapes in this study: these are the only type of data that are numerous enough to offer good spatial coverage and seasonal definition, due to the ease and low financial costs of sample collection and analysis. By compiling data from a large number

of sources and across numerous years and including "year" as a variance term within the INLA model, we hope to have accounted for some of the short-term POM variance.

Acidification of POM samples is recommended in the marine settings to remove carbonates that could affect $\delta^{13}C$ values, although the impact may be relatively low compared to spatial variance in $\delta^{13}C$ values at ocean basin scales (Lorrain et al., 2003). In this study, over 90% of the included samples were acidified and any potential effect was indirectly taken into account in the model via the random effect of "study." Development of common sampling protocols across research fields will improve efficiency of future modeling efforts.

Primary consumers such as zooplankton may be more appropriate for the generation of isotopic baselines (as a proxy for trophic level two) as they represent a more integrated isotopic signal over space and time, which may be less variable and thus more robust for applications such as animal migration studies. Zooplankton have previously been used to generate carbon and nitrogen isoscapes in regional studies including the Southern Ocean (Graham et al., 2010; McMahon et al., 2013; Troina et al., 2020; Yang et al., 2021). For this study, however, producing isoscapes based on zooplankton stable isotope values would have resulted in large unsampled areas, and therefore large uncertainties in modeled data. Furthermore, there is no consistency in the species or groups of zooplankton used, which complicates modeling due to variability in, for example, tissue turnover rates, fractionation, and trophic level (Pakhomov et al., 2019). Analysis of repeated latitudinal transects across the Southern Ocean has demonstrated that POM stable isotope values tend to be homogenous across space and time between fronts and associated cross water exchanges created by eddies (Espinasse et al., 2019). Overall, it is therefore reasonable to conclude that the high spatial variability predicted in stable isotope values overwhelms the potential variability associated with local changes in POM composition.

5. Conclusions

We characterized spatial and temporal variability in the isotopic composition of carbon and nitrogen in POM across the Southern Ocean in greater detail and coverage than it has previously been achieved. We identified broad spatial and seasonal structure in the recovered isoscape models, providing key evidence for explaining seasonal changes in biogeochemical processes and important implications for using isoscapes for animal assignment applications. We demonstrated that data from numerous sources and years can be combined and modeled to demonstrate these seasonal variabilities. However, the choice of statistical model has substantial impacts on the resultant spatial prediction and associated variability, as well as influencing how isoscape models can be used for future applications. The most accurate isoscape models included first-order interactions among the driving variables and were able to predict seasonal isotopic differences in regions with high sampling effort. However, they were associated with higher variability, due to the extrapolation of statistical relationships, relevant in open ocean sectors and in winter months where data are lacking. To improve isoscape accuracy and spatial precision to be able to detect mesoscale features such as eddies, more data are required over further temporal and spatial resolutions. Recognizing the paucity of zooplankton stable isotopic values in the Southern Ocean, future studies should focus on building a unified zooplankton stable isotope data base to supplement the POM-based isoscape modeling efforts.

Data Availability Statement

All POM carbon and nitrogen isotope data are available in Data Set S1 and are uploaded as a csv file to the data repository: https://github.com/KatieSJG/SO_isoscape.git. Mean and variance carbon and nitrogen isoscape predictions for both interaction and no-interaction models and for both annual average and seasonal predictions are saved as raster files and as csv files in the same repository. Environmental data raster surfaces used for these predictions are also uploaded. The R code used to perform the INLA isoscape predictions is also included. Additionally, the isoscapes and variance predictions produced in the present study are available on PANGAEA Data Publisher as raster files in 2° latitude by 1° longitude resolution (https://doi.org/10.1594/PANGAEA.934368).

Acknowledgments
POM data provided by NIWA were collected on RV Tangaroa (TAN) voyages by S. Bury, S. Nodder, A. Gutiérrez-Rodríguez, and K. Safi. Funding for sample collection and analysis was provided by the New Zealand Ministry of Business, Innovation and Employment and predecessor science funding agencies, including the Strategic Science Investment Fund to NIWA and the National Coasts & Oceans Centre. Stable isotope analyses from TAN voyages were carried out at the Environmental and Ecological Stable Isotope Facility, NIWA, Wellington, by A. Kilimnik and J. Delgado. Sample collection during the ANT voyages was done on board the RV "Polarstern" with assistance from M. Brener and L. Gurney. The surveys were financially supported by the German LAKRIS Project (Bundesministerium für Bildung und Forschung, BMBF Forschungsvorhaben 03F0406A/B) and the University of British Columbia (Canada). B. Hunt was funded from the European Union's Seventh Framework Programme under grant agreement no. 302010 (project ISOZOO) and Natural Sciences and Engineering Research Council of Canada grant RGPIN-2017-04499. MOBYDICK data sampling was supported by the French oceanographic fleet ("Flotte océanographique française"), ANR program (MOBYDICK project number: ANR-17-CE01-0013), and the research program of INSU-CNRS LEFE/CYBER ("Les enveloppes fluides et l'environnement"—"Cycles biogéochimiques, environnement et ressources"). POM data provided by Stanford University (R. Dunbar) were collected on voyages of the US NSF-operated RVIB Laurence M. Gould and Nathaniel B. Palmer between 1998 and 2002. All analyses were completed in the Stanford University Stable Isotope Biogeochemistry Laboratory with funding from NSF grants OPP-9615668, OPP-9909837, OPP-0207305, and OPP-1142044 (all to R. Dunbar). This project is supported in part by the Hong Kong Branch of Southern Marine Science and Engineering Guangdong Laboratory (Guangzhou; SMSEGL20SC02). B. Espinasse is funded from the European Union's Horizon 2020 MSCA program under grant agreement no. 894296—Project ISOMOD. K.

References

Altabet, M. A., & Francois, R. (1994). Sedimentary nitrogen isotopic ratio as a recorder for surface ocean nitrate utilization. *Global Biogeochemical Cycles*, *8*(1), 103–116. https://doi.org/10.1029/93GB03396

Arteaga, L. A., Boss, E., Behrenfeld, M. J., Westberry, T. K., & Sarmiento, J. L. (2020). Seasonal modulation of phytoplankton biomass in the Southern Ocean. *Nature Communications*, *11*(1), 5364. https://doi.org/10.1038/s41467-020-19157-2

Barrera, F., Lara, R. J., Krock, B., Garzón-Cardona, J. E., Fabro, E., & Koch, B. P. (2017). Factors influencing the characteristics and distribution or surface organic matter in the Pacific–Atlantic connection. *Journal of Marine Systems*, *175*, 36–45. https://doi.org/10.1016/j.jmarsys.2017.07.004

Behrenfeld, M. J., & Falkowski, P. G. (1997). Photosynthetic rates derived from satellite-based chlorophyll concentration. *Limnology & Oceanography*, *42*(1), 1–20. https://doi.org/10.4319/lo.1997.42.1.0001

Bentaleb, I., Fontugne, M., Descolas-Gros, C., Girardin, C., Mariotti, A., Pierre, C., et al. (1998). Carbon isotopic fractionation by plankton in the Southern Indian Ocean: Relationship between $\delta^{13}C$ of particulate organic carbon and dissolved carbon dioxide. *Journal of Marine Systems*, *17*(1–4), 39–58. https://doi.org/10.1016/s0924-7963(98)00028-1

Blain, S., Quéguiner, B., Armand, L., Belviso, S., Bombled, B., Bopp, L., et al. (2007). Effect of natural iron fertilization on carbon sequestration in the Southern Ocean. *Nature*, *446*, 1070–1074. https://doi.org/10.1038/nature05700

Bowen, G. J. (2010). Isoscapes: Spatial pattern in isotopic biogeochemistry. *Annual Review of Earth and Planetary Sciences*, *38*, 161–187. https://doi.org/10.1146/annurev-earth-040809-152429

Bowen, G. J., & Revenaugh, J. (2003). Interpolating the isotopic composition of modern meteoric precipitation. *Water Resources Research*, *39*(10), 1299. https://doi.org/10.1029/2003WR002086

Boyd, P. W., Watson, A. J., Law, C. S., Abraham, E. R., Trull, T., Murdoch, R., et al. (2000). A mesoscale phytoplankton bloom in the polar Southern Ocean stimulated by iron fertilization. *Nature*, *407*(6805), 695–702. https://doi.org/10.1038/35037500

Bracher, A. U., Kroon, B. M. A., & Lucas, M. I. (1999). Primary production, physiological state and composition of phytoplankton in the Atlantic Sector of the Southern Ocean. *Marine Ecology Progress Series*, *190*, 1–16. https://doi.org/10.3354/meps190001

Brault, E. K., Koch, P. L., McMahon, K. W., Broach, K. H., Rosenfield, A. P., Sauthoff, W., et al. (2018). Carbon and nitrogen zooplankton isoscapes in West Antarctica reflect oceanographic transitions. *Marine Ecology Progress Series*, *593*, 29–45. https://doi.org/10.3354/meps12524

Bucciarelli, E., Blain, S., & Tréguer, P. (2001). Iron and manganese in the wake of the Kerguelen Islands (Southern Ocean). *Marine Chemistry*, *73*(1), 21–36. https://doi.org/10.1016/s0304-4203(00)00070-0

Carreto, J. I., Montoya, N. G., Carignan, M. O., Akselman, R., Acha, E. M., & Derisio, C. (2016). Environmental and biological factors controlling the spring phytoplankton bloom at the Patagonian shelf-break front—Degraded fucoxanthin pigments and the importance of microzooplankton grazing. *Progress in Oceanography*, *146*, 1–21. https://doi.org/10.1016/j.pocean.2016.05.002

Ceia, F. R., Ramos, J. A., Phillips, R. A., Cherel, Y., Jones, D. C., Vieira, R. P., & Xavier, J. C. (2015). Analysis of stable isotope ratios in blood of tracked wandering albatrosses fails to distinguish a $\delta^{13}C$ gradient within their winter foraging areas in the southwest Atlantic Ocean. *Rapid Communications in Mass Spectrometry*, *29*(24), 2328–2336. https://doi.org/10.1002/rcm.7401

Cherel, Y., & Hobson, K. A. (2007). Geographical variation in carbon stable isotope signatures of marine predators: A tool to investigate their foraging areas in the Southern Ocean. *Marine Ecology Progress Series*, *329*, 281–287. https://doi.org/10.3354/meps329281

Darnaude, A. M., & Hunter, E. (2018). Validation of otolith $\delta^{18}O$ values as effective natural tags for shelf-scale geolocation of migrating fish. *Marine Ecology Progress Series*, *598*, 167–185. https://doi.org/10.3354/meps12302

de Baar, H. J. W., de Jong, J. T. M., Bakker, D. C. E., Löscher, B. M., Veth, C., Bathmann, U., & Smetacek, V. (1995). Importance of iron for plankton blooms and carbon dioxide drawdown in the Southern Ocean. *Nature*, *373*, 412–415. https://doi.org/10.1038/373412a0

Dehairs, F., Kopczynska, E., Nielsen, P., Lancelot, C., Bakker, D., Koeve, W., & Goeyens, L. (1997). $\delta^{13}C$ of Southern Ocean suspended organic matter during spring and early summer: Regional and temporal variability. *Deep Sea Research Part II: Topical Studies in Oceanography*, *44*(1–2), 129–142. https://doi.org/10.1016/s0967-0645(96)00073-2

Deniro, M. J., & Epstein, S. (1981). Influence of diet on the distribution of nitrogen isotopes in animals. *Geochimica et Cosmochimica Acta*, *45*(3), 341–351. https://doi.org/10.1016/0016-7037(81)90244-1

Deppeler, S. L., & Davidson, A. T. (2017). Southern Ocean phytoplankton in a changing climate. *Frontiers in Marine Science*, *4*, 40. https://doi.org/10.3389/fmars.2017.00040

Deuser, W. G. (1970). Isotopic evidence for diminishing supply of available carbon during diatom bloom in the Black Sea. *Nature*, *225*(5237), 1069–1071. https://doi.org/10.1038/2251069a0

DiFiore, P. J., Sigman, D. M., Karsh, K. L., Trull, T. W., Dunbar, R. B., & Robinson, R. S. (2010). Poleward decrease in the isotope effect of nitrate assimilation across the Southern Ocean. *Geophysical Research Letters*, *37*, L17601. https://doi.org/10.1029/2010GL044090

Durack, P. J., & Wijffels, S. E. (2010). Fifty-year trends in global ocean salinities and their relationship to broad-scale warming. *Journal of Climate*, *23*(16), 4342–4362. https://doi.org/10.1175/2010JCLI3377.1

Eadie, B. J., & Jeffrey, L. M. (1973). $\delta^{13}C$ analyses of oceanic particulate organic matter. *Marine Chemistry*, *1*(3), 199–209. https://doi.org/10.1016/0304-4203(73)90004-2

El-Sabaawi, R. W., Trudel, M., Mackas, D. L., Dower, J. F., & Mazumder, A. (2012). Interannual variability in bottom-up processes in the upstream range of the California Current system: An isotopic approach. *Progress in Oceanography*, *106*, 16–27. https://doi.org/10.1016/j.pocean.2012.06.004

Eppley, R. W. (1972). Temperature and phytoplankton growth in the sea. *Fishery Bulletin*, *70*, 1063–1085.

Espinasse, B., Hunt, B. P., Batten, S. D., & Pakhomov, E. A. (2020). Defining isoscapes in the Northeast Pacific as an index of ocean productivity. *Global Ecology and Biogeography*, *29*(2), 246–261. https://doi.org/10.1111/geb.13022

Espinasse, B., Pakhomov, E. A., Hunt, B. P. V., & Bury, S. J. (2019). Latitudinal gradient consistency in carbon and nitrogen stable isotopes of particulate organic matter in the Southern Ocean. *Marine Ecology Progress Series*, *631*, 19–30. https://doi.org/10.3354/meps13137

Francois, R., Altabet, M. A., Goericke, R., McCorkle, D. C., Brunet, C., & Poisson, A. (1993). Changes in the $\delta^{13}C$ of surface water particulate organic matter across the subtropical convergence in the SW Indian Ocean. *Global Biogeochemical Cycles*, *7*(3), 627–644. https://doi.org/10.1029/93GB01277

Franks, P. J. S. (2015). Has Sverdrup's critical depth hypothesis been tested? Mixed layers vs. turbulent layers. *ICES Journal of Marine Science*, *72*(6), 1897–1907. https://doi.org/10.1093/icesjms/fsu175

Fripiat, F., Sigman, D. M., Fawcett, S. E., Rafter, P. A., Weigand, M. A., & Tison, J. L. (2014). New insights into sea ice nitrogen biogeochemical dynamics from the nitrogen isotopes. *Global Biogeochemical Cycles*, *28*, 115–130. https://doi.org/10.1002/2013GB004729

Giménez, E. M., Winkler, G., Hoffmeyer, M., & Ferreyra, G. A. (2018). Composition, spatial distribution, and trophic structure of the zooplankton community in San Jorge Gulf, southwestern Atlantic Ocean. *Oceanography*, *31*(4), 154–163. https://doi.org/10.5670/oceanog.2018.418

Goericke, R., & Fry, B. (1994). Variations of marine plankton $\delta^{13}C$ with latitude, temperature, and dissolved CO_2 in the world ocean. *Global Biogeochemical Cycles*, *8*(1), 85–90. https://doi.org/10.1029/93GB03272

Graham, B. S., Koch, P. L., Newsome, S. D., McMahon, K. W., & Aurioles, D. (2010). Using isoscapes to trace the movements and foraging behavior of top predators in oceanic ecosystems. In J. B. West, G. J. Bowen, T. E. Dawson, & K. P. Tu (Eds.), *Isoscapes: Understanding movement, pattern, and process on Earth through isotope mapping* (pp. 299–318). Dordrecht, The Netherlands: Springer. https://doi.org/10.1007/978-90-481-3354-3_14

Gruber, N., Keeling, C. D., Bacastow, R. B., Guenther, P. R., Lueker, T. J., Wahlen, M., et al. (1999). Spatiotemporal patterns of carbon-13 in the global surface oceans and the oceanic Suess effect. *Global Biogeochemical Cycles*, *13*(2), 307–335. https://doi.org/10.1029/1999GB900019

Guinehut, S., Dhomps, A. L., Larnicol, G., & Le Traon, P. Y. (2012). High resolution 3-D temperature and salinity fields derived from in situ and satellite observations. *Ocean Science*, *8*(5), 845–857. https://doi.org/10.5194/os-8-845-2012

Henley, S. F., Cavan, E. L., Fawcett, S. E., Kerr, R., Monteiro, T., Sherrell, R. M., et al. (2020). Changing biogeochemistry of the Southern Ocean and its ecosystem implications. *Frontiers in Marine Science*, *7*, 581. https://doi.org/10.3389/fmars.2020.00581

Hofmann, M., Wolf-Gladrow, D. A., Takahashi, T., Sutherland, S. C., Six, K. D., & Maier-Reimer, E. (2000). Stable carbon isotope distribution of particulate organic matter in the ocean: A model study. *Marine Chemistry*, *72*(2), 131–150. https://doi.org/10.1016/s0304-4203(00)00078-5

Horii, S., Takahashi, K., Shiozaki, T., Hashihama, F., & Furuya, K. (2018). Stable isotopic evidence for the differential contribution of diazotrophs to the epipelagic grazing food chain in the mid-Pacific Ocean. *Global Ecology and Biogeography*, *27*(12), 1467–1480. https://doi.org/10.1111/geb.12823

Hussey, N. E., MacNeil, M. A., McMeans, B. C., Olin, J. A., Dudley, S. F. J., Cliff, G., et al. (2014). Rescaling the trophic structure of marine food webs. *Ecology Letters*, *17*(2), 239–250. https://doi.org/10.1111/ele.12226

Jaeger, A., Lecomte, V. J., Weimerskirch, H., Richard, P., & Cherel, Y. (2010). Seabird satellite tracking validates the use of latitudinal isoscapes to depict predators' foraging areas in the Southern Ocean. *Rapid Communications in Mass Spectrometry*, *24*(23), 3456–3460. https://doi.org/10.1002/rcm.4792

Jennings, S., & Warr, K. J. (2003). Environmental correlates of large-scale spatial variation in the $\delta^{15}N$ of marine animals. *Marine Biology*, *142*(6), 1131–1140. https://doi.org/10.1007/s00227-003-1020-0

Kennedy, H., & Robertson, J. (1995). Variations in the isotopic composition of particulate organic carbon in surface waters along an 88°W transect from 67°S to 54°S. *Deep Sea Research Part II: Topical Studies in Oceanography*, *42*(4–5), 1109–1122. https://doi.org/10.1016/0967-0645(95)00069-3

Kennicutt, M. C., Chown, S. L., Cassano, J. J., Liggett, D., Massom, R., Peck, L. S., et al. (2014). Polar research: Six priorities for Antarctic science. *Nature News*, *512*(7512), 23–25. https://doi.org/10.1038/512023a

Klein, E. S., Hill, S. L., Hinke, J. T., Phillips, T., & Watters, G. M. (2018). Impacts of rising sea temperature on krill increase risks for predators in the Scotia Sea. *PLoS One*, *13*(1), e0191011. https://doi.org/10.1371/journal.pone.0191011

Kline, T. C., Jr. (2009). Characterization of carbon and nitrogen stable isotope gradients in the northern Gulf of Alaska using terminal feed stage copepodite-V *Neocalanus cristatus*. *Deep Sea Research Part II: Topical Studies in Oceanography*, *56*(24), 2537–2552. https://doi.org/10.1016/j.dsr2.2009.03.004

Kurle, C. M., & McWhorter, J. K. (2017). Spatial and temporal variability within marine isoscapes: Implications for interpreting stable isotope data from marine systems. *Marine Ecology Progress Series*, *568*, 31–45. https://doi.org/10.3354/meps12045

Lannuzel, D., Chever, F., van der Merwe, P. C., Janssens, J., Roukaerts, A., Cavagna, A.-J., et al. (2016). Iron biogeochemistry in Antarctic pack ice during SIPEX-2. *Deep Sea Research Part II: Topical Studies in Oceanography*, *131*, 111–122. https://doi.org/10.1016/j.dsr2.2014.12.003

Lara, R. J., Alder, V., Franzosi, C. A., & Kattner, G. (2010). Characteristics of suspended particulate organic matter in the southwestern Atlantic: Influence of temperature, nutrient and phytoplankton features on the stable isotope signature. *Journal of Marine Systems*, *79*(1), 199–209. https://doi.org/10.1016/j.jmarsys.2009.09.002

Laws, E. A., Bidigare, R. R., & Popp, B. N. (1997). Effect of growth rate and CO_2 concentration on carbon isotopic fractionation by the marine diatom *Phaeodactylum tricornutum*. *Limnology & Oceanography*, *42*(7), 1552–1560. https://doi.org/10.4319/lo.1997.42.7.1552

Lee, S. H., Schell, D. M., McDonald, T. L., & Richardson, W. J. (2005). Regional and seasonal feeding by bowhead whales *Balaena mysticetus* as indicated by stable isotope ratios. *Marine Ecology Progress Series*, *285*, 271–287. https://doi.org/10.3354/meps285271

Li, W. K., McLaughlin, F. A., Lovejoy, C., & Carmack, E. C. (2009). Smallest algae thrive as the Arctic Ocean freshens. *Science*, *326*(5952), 539–539. https://doi.org/10.1126/science.1179798

Loeb, V., Siegel, V., Holm-Hansen, O., Hewitt, R., Fraser, W., Trivelpiece, W., & Trivelpiece, S. (1997). Effects of sea-ice extent and krill or salp dominance on the Antarctic food web. *Nature*, *387*(6636), 897–900. https://doi.org/10.1038/43174

Lorrain, A., Savoye, N., Chauvaud, L., Paulet, Y.M., & Naulet, N. (2003). Decarbonation and preservation method for the analysis of organic C and N contents and stable isotope ratios of low-carbonated suspended particulate material. *Analytica Chimica Acta*, *491*(2), 125–133. https://doi.org/10.1016/s0003-2670(03)00815-8

Lourey, M. J., Trull, T. W., & Sigman, D. M. (2003). Sensitivity of $\delta^{15}N$ of nitrate, surface suspended and deep sinking particulate nitrogen to seasonal nitrate depletion in the Southern Ocean. *Global Biogeochemical Cycles*, *17*(3), 1081. https://doi.org/10.1029/2002GB001973

Lourey, M. J., Trull, T. W., & Tilbrook, B. (2004). Sensitivity of $\delta^{13}C$ of Southern Ocean suspended and sinking organic matter to temperature, nutrient utilization, and atmospheric CO_2. *Deep Sea Research Part I: Oceanographic Research Papers*, *51*(2), 281–305. https://doi.org/10.1016/j.dsr.2003.10.002

MacKenzie, K. M., Longmore, C., Preece, C., Lucas, C. H., & Trueman, C. N. (2014). Testing the long-term stability of marine isoscapes in shelf seas using jellyfish tissues. *Biogeochemistry*, *121*(2), 441–454. https://doi.org/10.1007/s10533-014-0011-1

Magozzi, S., Yool, A., Zanden, H. B. V., Wunder, M. B., & Trueman, C. N. (2017). Using ocean models to predict spatial and temporal variation in marine carbon isotopes. *Ecosphere*, *8*(5), e01763. https://doi.org/10.1002/ecs2.1763

Maritorena, S., d'Andon, O. H. F., Mangin, A., & Siegel, D. A. (2010). Merged satellite ocean color data products using a bio-optical model: Characteristics, benefits and issues. *Remote Sensing of Environment*, *114*(8), 1791–1804. https://doi.org/10.1016/j.rse.2010.04.002

Marshall, G. J. (2003). Trends in the southern annular mode from observations and reanalyses. *Journal of Climate*, *16*(24), 4134–4143. https://doi.org/10.1175/1520-0442(2003)016<4134:TITSAM>2.0.CO;2

Martin, J. H. (1990). Glacial–interglacial CO_2 change: The Iron Hypothesis. *Paleoceanography*, *5*(1), 1–13. https://doi.org/10.1029/PA005i001p00001

McMahon, K. W., Hamady, L. L., & Thorrold, S. R. (2013). A review of ecogeochemistry approaches to estimating movements of marine animals. *Limnology & Oceanography*, *58*(2), 697–714. https://doi.org/10.4319/lo.2013.58.2.0697

Mongin, M., Molina, E., & Trull, T. W. (2008). Seasonality and scale of the Kerguelen plateau phytoplankton bloom: A remote sensing and modeling analysis of the influence of natural iron fertilization in the Southern Ocean. *Deep Sea Research Part II: Topical Studies in Oceanography*, *55*, 880–892. https://doi.org/10.1016/j.dsr2.2007.12.039

Montecinos, S., Castro, L. R., & Neira, S. (2016). Stable isotope ($\delta^{13}C$ and $\delta^{15}N$) and trophic position of Patagonian sprat (*Sprattus fuegensis*) from the Northern Chilean Patagonia. *Fisheries Research*, *179*, 139–147. https://doi.org/10.1016/j.fishres.2016.02.014

Montoya, J. P., Carpenter, E. J., & Capone, D. G. (2002). Nitrogen fixation and nitrogen isotope abundances in zooplankton of the oligotrophic North Atlantic. *Limnology & Oceanography*, *47*(6), 1617–1628. https://doi.org/10.4319/lo.2002.47.6.1617

Morel, A. (1991). Light and marine photosynthesis: A spectral model with geochemical and climatological implications. *Progress in Oceanography*, *26*(3), 263–306. https://doi.org/10.1016/0079-6611(91)90004-6

Munro, D. R., Dunbar, R. B., Mucciarone, D. A., Arrigo, K. R., & Long, M. C. (2010). Stable isotope composition of dissolved inorganic carbon and particulate organic carbon in sea ice from the Ross Sea, Antarctica. *Journal of Geophysical Research: Oceans*, *115*, C09005. https://doi.org/10.1029/2009JC005661

O'Leary, T., Trull, T., Griffiths, F., Tilbrook, B., & Revill, A. (2001). Euphotic zone variations in bulk and compound-specific $\delta^{13}C$ of suspended organic matter in the Subantarctic Ocean, south of Australia. *Journal of Geophysical Research: Oceans*, *106*(C12), 31669–31684. https://doi.org/10.1029/2000JC000288

Orsi, A. H., & Harris, U. (2019). *Fronts of the Antarctic Circumpolar Current—GIS data*. Retrieved from https://data.aad.gov.au/metadata/records/antarctic_circumpolar_current_frontshttps://researchdata.edu.au/fronts-antarctic-circumpolar-current-gis

Pakhomov, E. A., Henschke, N., Hunt, B. P., Stowasser, G., & Cherel, Y. (2019). Utility of salps as a baseline proxy for food web studies. *Journal of Plankton Research*, *41*(1), 3–11. https://doi.org/10.1093/plankt/fby051

Pethybridge, H., Choy, C. A., Logan, J. M., Allain, V., Lorrain, A., Bodin, N., et al. (2018). A global meta-analysis of marine predator nitrogen stable isotopes: Relationships between trophic structure and environmental conditions. *Global Ecology and Biogeography*, *27*(9), 1043–1055. https://doi.org/10.1111/geb.12763

Popp, B. N., Trull, T., Kenig, F., Wakeham, S. G., Rust, T. M., Tilbrook, B., et al. (1999). Controls on the carbon isotopic composition of Southern Ocean phytoplankton. *Global Biogeochemical Cycles*, *13*(4), 827–843. https://doi.org/10.1029/1999GB900041

Post, D. M. (2002). Using stable isotopes to estimate trophic position: Models, methods, and assumptions. *Ecology*, *83*(3), 703–718. https://doi.org/10.1890/0012-9658(2002)083[0703:USITET]2.0.CO;2

Quillfeldt, P., Masello, J. F., McGill, R. A. R., Adams, M., & Furness, R. W. (2010). Moving polewards in winter: A recent change in the migratory strategy of a pelagic seabird? *Frontiers in Zoology*, *7*, 15. https://doi.org/10.1186/1742-9994-7-15

Rau, G. H., Low, C., Pennington, J. T., Buck, K. R., & Chavez, F. P. (1998). Suspended particulate nitrogen $\delta^{15}N$ versus nitrate utilization: Observations in Monterey Bay, CA. *Deep Sea Research Part II: Topical Studies in Oceanography*, *45*(8), 1603–1616. https://doi.org/10.1016/s0967-0645(98)80008-8

Rau, G., Takahashi, T., Des Marais, D., & Sullivan, C. (1991). Particulate organic matter $\delta^{13}C$ variations across the Drake Passage. *Journal of Geophysical Research*, *96*(C8), 15131–15135. https://doi.org/10.1029/91JC01253

Reiss, C. S., Cossio, A., Santora, J. A., Dietrich, K. S., Murray, A., Mitchell, B. G., et al. (2017). Overwinter habitat selection by Antarctic krill under varying sea-ice conditions: Implications for top predators and fishery management. *Marine Ecology Progress Series*, *568*, 1–16. https://doi.org/10.3354/meps12099

Riaux-Gobin, C., Fontugne, M., Jensen, K., Bentaleb, I., Cauwet, G., Chrétiennot-Dinet, M.-J., & Poisson, A. (2006). Surficial deep-sea sediments across the polar frontal system (Southern Ocean, Indian sector): Particulate carbon content and microphyte signatures. *Marine Geology*, *230*(3–4), 147–159. https://doi.org/10.1016/j.margeo.2006.04.005

Richoux, N. B., & Froneman, P. W. (2009). Plankton trophodynamics at the subtropical convergence, Southern Ocean. *Journal of Plankton Research*, *31*(9), 1059–1073. https://doi.org/10.1093/plankt/fbp054

Riebesell, U., Burkhardt, S., Dauelsberg, A., & Kroon, B. (2000). Carbon isotope fractionation by a marine diatom: Dependence on the growth-rate-limiting resource. *Marine Ecology. Progress Series*, *193*, 295–303. https://doi.org/10.3354/meps193295

Rogers, A., Frinault, B., Barnes, D., Bindoff, N., Downie, R., Ducklow, H., et al. (2020). Antarctic futures: An assessment of climate-driven changes in ecosystem structure, function, and service provisioning in the Southern Ocean. *Annual Review of Marine Science*, *12*, 87–120. https://doi.org/10.1146/annurev-marine-010419-011028

Rolff, C. (2000). Seasonal variation in $\delta^{13}C$ and $\delta^{15}N$ of size-fractionated plankton at a coastal station in the northern Baltic proper. *Marine Ecology Progress Series*, *203*, 47–65. https://doi.org/10.3354/meps203047

Rue, H., Martino, S., & Chopin, N. (2009). Approximate Bayesian inference for latent Gaussian models using integrated nested Laplace approximations (with discussion). *Journal of the Royal Statistical Society: Series B*, *71*, 319–392. https://doi.org/10.1111/j.1467-9868.2008.00700.x

Ryabenko, E. (2013). Stable isotope methods for the study of the nitrogen cycle. In E. Zambianchi (Ed.), *Topics in oceanography*. London: InTech. https://doi.org/10.5772/56105

Sakamoto, T., Komatsu, K., Shirai, K., Higuchi, T., Ishimura, T., Setou, T., et al. (2019). Combining microvolume isotope analysis and numerical simulation to reproduce fish migration history. *Methods in Ecology and Evolution*, *10*(1), 59–69. https://doi.org/10.1111/2041-210X.13098

Schmidt, K., Atkinson, A., Stübing, D., McClelland, J. W., Montoya, J. P., & Voss, M. (2003). Trophic relationships among Southern Ocean copepods and krill: Some uses and limitations of a stable isotope approach. *Limnology & Oceanography*, *48*(1), 277–289. https://doi.org/10.4319/lo.2003.48.1.0277

Schofield, O., Ducklow, H. W., Martinson, D. G., Meredith, M. P., Moline, M. A., & Fraser, W. R. (2010). How do polar marine ecosystems respond to rapid climate change? *Science*, *328*(5985), 1520–1523. https://doi.org/10.1126/science.1185779

Seyboth, E., Botta, S., Mendes, C. R. B., Negrete, J., Dalla Rosa, L., & Secchi, E. R. (2018). Isotopic evidence of the effect of warming on the northern Antarctic Peninsula ecosystem. *Deep Sea Research Part II: Topical Studies in Oceanography*, *149*, 218–228. https://doi.org/10.1016/j.dsr2.2017.12.020

Sokolov, S., & Rintoul, S. R. (2009). Circumpolar structure and distribution of the Antarctic Circumpolar Current fronts: 1. Mean circumpolar paths. *Journal of Geophysical Research*, *114*, C11018. https://doi.org/10.1029/2008JC005108

Somes, C. J., Schmittner, A., Galbraith, E. D., Lehmann, M. F., Altabet, M. A., Montoya, J. P., et al. (2010). Simulating the global distribution of nitrogen isotopes in the ocean. *Global Biogeochemical Cycles*, *24*, GB4019. https://doi.org/10.1029/2009GB003767

St John Glew, K., Graham, L. J., McGill, R. A., & Trueman, C. N. (2019). Spatial models of carbon, nitrogen and sulphur stable isotope distributions (isoscapes) across a shelf sea: An INLA approach. *Methods in Ecology and Evolution*, *10*, 518–531.

St John Glew, K., Wanless, S., Harris, M. P., Daunt, F., Erikstad, K. E., Strøm, H., & Trueman, C. N. (2018). Moult location and diet of auks in the North Sea inferred from coupled light-based and isotope-based geolocation. *Marine Ecology Progress Series*, *599*, 239–251. https://doi.org/10.3354/meps12624

Stowasser, G., Atkinson, A., McGill, R., Phillips, R., Collins, M. A., & Pond, D. (2012). Food web dynamics in the Scotia Sea in summer: A stable isotope study. *Deep Sea Research Part II: Topical Studies in Oceanography*, *59*, 208–221. https://doi.org/10.1016/j.dsr2.2011.08.004

Strutton, P., Lovenduski, N., Mongin, M., & Matear, R. (2012). Quantification of Southern Ocean phytoplankton biomass and primary productivity via satellite observations and biogeochemical models. *CCAMLR Science*, *19*, 247–265.

Swart, N. C., Gille, S. T., Fyfe, J. C., & Gillett, N. P. (2018). Recent Southern Ocean warming and freshening driven by greenhouse gas emissions and ozone depletion. *Nature Geoscience*, *11*(11), 836–841. https://doi.org/10.1038/s41561-018-0226-1

Switzer, A. C., Kamykowski, D., & Zentara, S. J. (2003). Mapping nitrate in the global ocean using remotely sensed sea surface temperature. *Journal of Geophysical Research*, *108*(C8), 3280. https://doi.org/10.1029/2000JC000444

Tagliabue, A., Bowie, A. R., Boyd, P. W., Buck, K. N., Johnson, K. S., & Saito, M. A. (2017). The integral role of iron in ocean biogeochemistry. *Nature*, *543*(7643), 51–59. https://doi.org/10.1038/nature21058

Trebilco, R., Melbourne-Thomas, J., & Constable, A. J. (2020). The policy relevance of Southern Ocean food web structure: Implications of food web change for fisheries, conservation and carbon sequestration. *Marine Policy*, *115*, 103832. https://doi.org/10.1016/j.marpol.2020.103832

Troina, G. C., Dehairs, F., Botta, S., Di Tullio, J. C., Elskens, M., & Secchi, E. R. (2020). Zooplankton-based $\delta^{13}C$ and $\delta^{15}N$ isoscapes from the outer continental shelf and slope in the subtropical western South Atlantic. *Deep Sea Research Part I: Oceanographic Research Papers*, *159*, 103235. https://doi.org/10.1016/j.dsr.2020.103235

Trueman, C. N., Jackson, A. L., Chadwick, K. S., Coombs, E. J., Feyrer, L. J., Magozzi, S., et al. (2019). Combining simulation modeling and stable isotope analyses to reconstruct the last known movements of one of Nature's giants. *PeerJ*, *7*, e7912. https://doi.org/10.7717/peerj.7912

Trueman, C. N., MacKenzie, K. M., & Palmer, M. R. (2012). Identifying migrations in marine fishes through stable-isotope analysis. *Journal of Fish Biology*, *81*(2), 826–847. https://doi.org/10.1111/j.1095-8649.2012.03361.x

Trueman, C. N., & St John Glew, K. (2019). Isotopic tracking of marine animal movement. In *Tracking animal migration with stable isotopes* (pp. 137–172). New York: Elsevier. https://doi.org/10.1016/b978-0-12-814723-8.00006-4

Trull, T., & Armand, L. (2001). Insights into Southern Ocean carbon export from the $\delta^{13}C$ of particles and dissolved inorganic carbon during the SOIREE iron release experiment. *Deep Sea Research Part II: Topical Studies in Oceanography*, *48*(11), 2655–2680. https://doi.org/10.1016/s0967-0645(01)00013-3

Wada, E., Terazaki, M., Kabaya, Y., & Nemoto, T. (1987). ^{15}N and ^{13}C abundances in the Antarctic Ocean with emphasis on the biogeochemical structure of the food web. *Deep Sea Research Part A. Oceanographic Research Papers*, *34*(5–6), 829–841. https://doi.org/10.1016/0198-0149(87)90039-2

Wunder, M. B. (2010). Using isoscapes to model probability surfaces for determining geographic origins. In J. B. West, G. J. Bowen, T. E. Dawson, & K. P. Tu (Eds.), *Isoscapes: Understanding movement, pattern, and process on Earth through isotope mapping* (pp. 251–270). Dordrecht, The Netherlands: Springer. https://doi.org/10.1007/978-90-481-3354-3_12

Yang, G., Atkinson, A., Hill, S. L., Guglielmo, L., Granata, A., & Li, C. (2021). Changing circumpolar distributions and isoscapes of Antarctic krill: Indo-Pacific habitat refuges counter long-term degradation of the Atlantic sector. *Limnology & Oceanography*, *66*(1), 272–287.

Zhang, R., Zheng, M., Chen, M., Ma, Q., Cao, J., & Qiu, Y. (2014). An isotopic perspective on the correlation of surface ocean carbon dynamics and sea ice melting in Prydz Bay (Antarctica) during austral summer. *Deep Sea Research Part I: Oceanographic Research Papers*, *83*, 24–33. https://doi.org/10.1016/j.dsr.2013.08.006